Simplified calculation method for coupled thermal–mechanical stress of drum using beam elements

Yanjun Li, Zhenhua Zhang, Qingpeng Zeng, Chenshuo Li, Jianxin Shi*, Guolei Zhang*

College of Power and Energy Engineering, Harbin Engineering University, Nantong Street, Harbin 150001, PR China

Abstract: The drum is the core part of a supercharged boiler that is prone to fatigue damage due to the dual action of thermal and mechanical stress. However, owing to its complex structure, complete modeling calculation of the drum requires considerable computational resources. Therefore, based on the basic theory of beam elements, we propose a simplified method using beam elements in place of solid tubes and evaluate the feasibility of this method. The results demonstrate that the simplified method reduced the overall mesh number of the model by 67.19% and the calculation time by 68.08%. Moreover, compared to the solid model, the maximum relative errors of stress and displacement were only 3.44% and 5.16%. Considering the dispersion of low-cycle fatigue life, we applied a statistical approach to the fatigue life assessment of the drum, and obtained the probability of failure corresponding to the fatigue life of the drum under the given operating conditions. This method provides an important basis for the systematic evaluation of fatigue life under various operating conditions and the prediction of failure occurrence.

Keywords: boiler drum; beam element; simplified method; statistics; fatigue life.

* Corresponding author. Fax: +86-0451-82519305

E-mail address: shijianxin@hrbeu.edu.cn (J.X. SHI)

zhangguolei@hrbeu.edu.cn (GL.ZHANG)

1 Introduction

A boiler is an energy conversion and waste heat recovery vessel that is widely used in power stations, shipbuilding, metallurgy, chemical and textile industries, etc[1]. Based on the air supply method of the furnace, boilers can be divided into atmospheric boilers and supercharged boilers. Supercharged boilers use compressed air generated by a compressor in place of the steam turbine blower of an atmospheric boiler to deliver combustion-supporting air to the furnace. Compared to atmospheric boilers, supercharged boilers have a larger volumetric heat load and heat transfer intensity, and offer several advantages in terms of weight and volume. Owing to their superior reliability, maneuverability, maintainability, and economic performance, supercharged boilers have gradually replaced atmospheric boilers for power production on large ships[2]. However, although there is a significant amount of research on the heat transfer and mechanical properties of

atmospheric boiler drums, studies on supercharged boilers are relatively few. The drum is the core pressure component of a supercharged boiler. It is used to generate high temperature, high pressure steam, and store the boiler water. During the operation of a supercharged boiler, such as during start-up, shut-down, and load lifting, the pressure and temperature of the fluid in the drum can change significantly in a short amount of time. Consequently, the boiler drum is prone to fatigue failure due to the combined action of the frequent fluctuations in the mechanical and thermal stress. Therefore, a coupled thermal–mechanical analysis of the drum is of significant importance to accurately predict its fatigue life.

Owing to the complexity of the boiler structure, it is usually simplified to varying degrees in related studies. Saha et al.[3] used finite element software to analyze the structure of the drum under internal pressure. Considering the symmetry of the model, only half the model was analyzed. They revealed that metallurgical factors and operating conditions were the main reasons for the damage caused to the drum. Juan et al.[4] simplified the calculation process by only considering half of the steam drum along the axial direction for modeling and analysis, and only retaining the pipe holes while ignoring the influence of the pipe bundle. Furthermore, they performed a transient thermo–mechanical analysis of the boiler drum using the data measured during the start-up process of a power plant boiler as the boundary condition. The results demonstrated that the operating status of the boiler has a direct impact on the fatigue life of the steam drum. Okrajni[5] used a certain type of pressure vessel as the research object and used the vertical plane as the symmetric plane for finite element calculations. Equal and reverse uniform loads were applied on both sides of the drum to simulate the axial force due to internal pressure, and elastic restraints were applied to the bottom end of the tube. The stress distribution indicated that a stress concentration area exists near the hole, leading to the fatigue failure of the drum. Andrzej et al.[6] believed that the drum wall temperature only changes along the radial direction of the drum. Therefore, they simplified the drum as a two-dimensional structure for temperature field calculations. In addition, considering the changes in stress along the circumferential, axial, and radial directions, they performed stress calculations using a three-dimensional structure. Qingpeng Zeng et al. [7] analyzed the complete modeling of supercharged boilers, but in order to reduce the requirements for computer performance. When the tube bundle is meshed, a coarser mesh size is used, and the accuracy of the calculation results still needs to be improved.

The research discussed above is primarily based on simplifying the calculation process and does not model the structure of certain non-key areas. Although this improves the calculation efficiency to some extent, these simplification methods completely ignore the interactions between structures, and the reliability of the calculation results are questionable. Therefore, in this study, we aim to establish a simplified research method using beam elements in place of boiler tubes to reduce the calculation costs, while ensuring the accuracy of the structural analysis. This method has numerous applications in various fields. Sreenath et al.[8] used beam–shell hybrid elements and full shells to model and analyze steel structures. The beam elements were the main body of the steel structure, and the shell elements were used to model the bending part. The calculation error of the resulting beam–shell hybrid structure was only 0.91%, and the calculation time was reduced by 83%. Adam et al.[9] used a beam–shell hybrid structure to simplify the modeling and analysis of the support towers of wind turbines. They replaced most of the strakes with beam element structures, and shell element structures were only used to model the area of interest. Such modeling methods can significantly improve the calculation efficiency of finite element

simulation, despite reducing the calculation accuracy. The relevant calculation efficacy was proved by designing a 1.5 MW wind turbine. Sanghoon Lee et al.[10] used beam element structures for the impact simulation calculation of fuel rods. The fuel rods containing fuel pellets, cladding layer, and bonding layer were simplified as a homogeneous isotropic beam. The calculation results demonstrated that this method performs well when the fuel rod is subjected to horizontal and vertical loads. Kim[11] proposed a simplified hybrid finite element model composed of solid elements and beam elements for the fatigue assessment of the level 1 components of nuclear power plants under severe seismic loads. The solid elements were used in areas where plastic behavior was expected due to high stress and strain, and the beam elements were used in areas where elastic behavior was expected. The results indicated that this structure simplification method could provide reasonable and conservative results. In several studies[12–14], the basic theory of beam elements has been used to derive suitable beam element models based on their specific application environment. These studies have provided subsequent researchers with numerous types of beam elements.

This paper presents a simplified research method wherein the boiler bundle is replaced with beam units to calculate and analyze the thermal–mechanical coupling of boiler tubes. A fatigue statistical method is used to evaluate the fatigue life of the drum considering the dispersion of low-cycle fatigue life and other factors. The proposed method improves the structural analysis and fatigue life evaluation of the boiler barrel of a supercharged boiler, and improves the reliability of the structural analysis calculation and the accuracy of the fatigue life prediction of low-cycle fatigue. It provides a basis for the study of simplified methods for large-scale heat exchange equipment and fatigue life evaluation.

2 Mathematical Model

2.1 Thermal stress

The thermal stress generated by the drum in the radial, axial, and tangential directions is calculated as:

$$\sigma_{\theta}^{t} = \frac{aE\Delta t}{2(1-\mu)}\left(\frac{1-\ln K_r}{\ln K} - \frac{K_r^2+1}{K^2-1}\right) \tag{1}$$

$$\sigma_{r}^{t} = \frac{aE\Delta t}{2(1-\mu)}\left(\frac{\ln K_r}{\ln K} + \frac{K_r^2-1}{K^2-1}\right) \tag{2}$$

$$\sigma_{z}^{t} = \frac{aE\Delta t}{2(1-\mu)}\left(\frac{1-2\ln K_r}{\ln K} - \frac{2}{K^2-1}\right) \tag{3}$$

2.2 Mechanical stress

The internal pressure of the drum is due to high-pressure steam, and the external pressure is approximately equal to the atmospheric pressure. The large pressure difference between the interior and exterior of the drum enables it to withstand significant mechanical stress, which cannot be ignored in the fatigue life analysis of the material. The mechanical stress of the drum due to internal and external pressure can be calculated using Lame's formula:

$$\sigma_{r}^{s} = \frac{r_1^2}{r_2^2-r_1^2}\left(1-\frac{r_2^2}{r^2}\right)p_i - \frac{r_2^2}{r_2^2-r_1^2}\left(1-\frac{r_1^2}{r^2}\right)p_0 \tag{4}$$

$$\sigma_\theta^s = \frac{r_1^2}{r_2^2 - r_1^2}\left(1 + \frac{r_2^2}{r^2}\right)p_i - \frac{r_2^2}{r_2^2 - r_2^2}\left(1 + \frac{r_1^2}{r^2}\right)p_0 \tag{5}$$

$$\sigma_z^s = \frac{p_i r_1^2 - p_0 r_2^2}{r_2^2 - r_1^2} \tag{6}$$

This formula is applicable to any wall thickness problem.

2.3 Timoshenko beam theory

The first-order shear deformation theory based on Timoshenko beam theory is used to simplify the tube of the supercharged boiler. The simplified tube element type used herein is PIPE288, as shown in **Fig. 1**. This element is suitable for medium thickness (1.5–3.0 mm) pipes. The relevant calculation theory is shown below[15]:

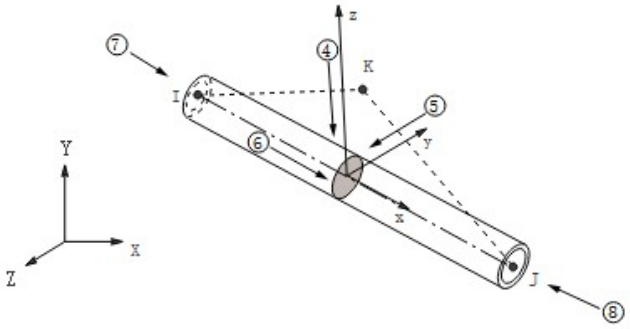

Fig. 1 Schematic diagram of PIPE288 element

1) Geometric equations:

The rotation angle of the beam axis is:

$$\varphi = \frac{dw}{dx} \tag{7}$$

The equation of the rotation angle is:

$$\varphi = \theta + \gamma \tag{8}$$

Section curvature:

$$\kappa = \frac{d\theta}{dx} \tag{9}$$

2) Equilibrium equations:

Moment balance equation:

$$\frac{dM(x)}{dx} = -V(x) \tag{10}$$

Shear balance equation:

$$\frac{dV(x)}{dx} = -q_y(x) \tag{11}$$

3) Physical equations:

The bending stiffness is:

$$M(x) = EI \cdot \kappa \tag{12}$$

The shear stiffness is:

$$V(x) = \frac{GA\gamma}{k} \tag{13}$$

4) Deflection governing equation:

Using equations (10)–(12):

$$EI\frac{d^2k}{dx^2} = q_y(x) \tag{14}$$

Using equations (7)–(9) and equation (13):

$$\frac{d^2k}{dx^2} = \frac{d^4v}{dx^4} + \frac{k}{GA}\frac{d^2q_y(x)}{dx^2} \tag{15}$$

The deflection governing equation can be obtained by combining equations (14) and (15).

$$\frac{d^4v}{dx^4} = \frac{q_y(x)}{EI} - \frac{k}{GA}\frac{d^2q_y(x)}{dx^2} \tag{16}$$

5) Shear angle governing equation:

$$\frac{d\gamma}{dx} = -\frac{kq_y(x)}{GA} \tag{17}$$

6) Displacement coordination equation:

The coordination equation of the deflection and shear angle can be obtained from equations (7)–(14).

$$\frac{d^2\gamma}{dx^2} = \frac{d^3v}{dx^3} + \frac{GA\gamma}{EIk} \tag{18}$$

2.4 Calculation of fatigue life

Supercharged boilers are pressure vessels, and their fatigue failure process is low-cycle fatigue. The fatigue life calculation method is as follows[16].

$$Y = \log[28.3E3(\frac{S_a}{E_T})] \tag{19}$$

$$X = -4706.5245 + 1813.6228Y + \frac{6785.5644}{Y} - 368.12404Y^2 - \frac{5133.7345}{Y^2} + 30.708204Y^3 + \frac{1596.1916}{Y^3}(10^Y \quad 20) \tag{20}$$

$$X = \frac{38.1309 - 60.1705Y^2 + 25.0352Y^4}{1 + 1.80224Y^2 - 4.68904Y^4 + 2.26536Y^6}(10^Y < 20) \tag{21}$$

$$N = 10^X \tag{22}$$

The above formula is only applicable when the material is carbon low alloy 4XX series high-alloy steel, with high tensile strength at temperatures below 371℃, and a minimum ultimate

tensile strength of less than 552 MPa.

2.5 Multi-point constraint (MPC) contact

Considering the special structure of a beam–solid contact surface, the MPC (Multi-Point Constraint) binding contact method is adopted herein. The MPC contact method defines the coupling relationship between the degrees of freedom of the nodes using the Lagrange multiplier method. Subsequently, a relationship is established between certain degrees of freedom of other designated nodes, and this standard value is based on the constraint equation. The MPC is used to characterize specific physical phenomena, such as rigid connections, hinges, sliding, etc., and can be used to describe the load transfer between incompatible units. This method not only constrains translational freedom, but also restrains rotational freedom, improves the accuracy of the solution, and makes the connection between the beam and the solid more reasonable. The constraint equation between the node degrees of freedom is[17]:

$$u_i + \sum_{j=1}^{n} C_j u_j = C_0 \tag{23}$$

3 Physical Model

3.1 Model introduction

Several tubes such as downcomers, convection heat exchange tubes, and superheat tubes are installed in the orifice plate of the supercharged boiler drum to complete the steam–water cycle，as shown in **Fig 2(a)**. The contact between the orifice plate and the tubes is affected by the combined effects of the thermal stress and the mechanical stress, as well as the interaction forces between the two. Consequently, this area is most prone to fatigue failure. The modeling of these tubes is extremely important to study the fatigue failure of the drum. However, if each tube is modeled and analyzed individually, the numerical calculation cost increases significantly. Moreover, owing to the relatively large number of meshes in the tubes, a detailed analysis of the stress concentration areas such as the orifice plate cannot be performed. Therefore, most scholars neglect the tubes and adopt various assumptions for equivalent modeling. The inner and outer diameters, length, and bending mode of the tubes have a significant impact on the orifice plate under the action of various forces (thermal and mechanical stress). Consequently, simply ignoring the tubes does not accurately reflect the true stress of the orifice plate. To ensure the efficiency and accuracy of this research, we propose the following assumptions:

1 The weight of the working fluid and the structure is ignored;

2 The effects of the furnace wall and guard plate on the tube and drum are ignored;

3 The functions of the lower and superheater headers are ignored.

Fig. 2(b) shows the physical model of the supercharged boiler established herein. The drum and tubes are made of Q245R steel, which has good mechanical properties and corrosion resistance, and is commonly used in pressure vessels.

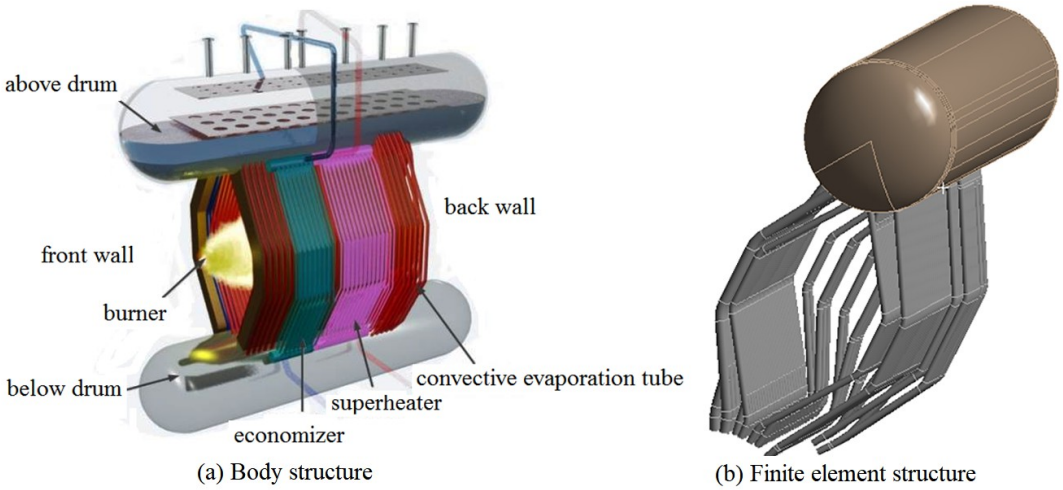

Fig. 2 Supercharged boiler stucture

3.2 Simplified tube model

To address the problems mentioned in the previous section, we propose a simplified method of replacing a part of the tubes with beam elements, as shown in **Fig. 3**. The beam element is a special type of structure that is completely composed of edges and has no surface area or volume but can achieve mechanical properties similar to solid parts by defining a cross-section type.

In the simplified method, a beam–solid hybrid structure is used to model the boiler tubes, and the cross-sections of the beam element tubes are defined based on the inner and outer diameters of the solid tubes. The mechanical properties of the beam element tubes and the solid tubes are similar—they can both withstand axial tension, compression, bending, and torsion[11]—and can be used to define the internal and external pressure and temperature of the pipe. This results in significant time savings for modeling and meshing , compared to solid elements, the time required for the meshing of beam elements is negligible. The boundary conditions of the simplified model are consistent with those of the solid model, and the calculation results of the solid model can be used as a reference to evaluate the simplification effect of the simplified model.

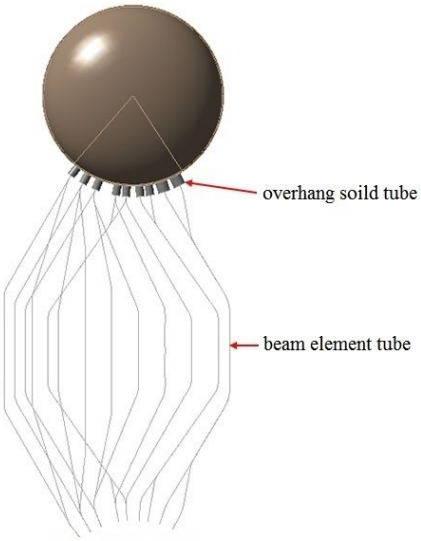

Fig. 3 Solid and simplified model

4 Operating conditions

The heat exchange method between each wall of the supercharged boiler differs significantly. In this study, we divide the area according to the actual heat exchange situation in the drum, as

shown in **Fig. 4**. The area AB is the left side of the boiler that is responsible for convective heat exchange with the air, BC is the furnace wall and insulation layer coverage area, CF is the furnace radiant heat exchange area, FG is the furnace wall and insulation layer coverage area, and GH is the flue gas convection exchange area, HI is the furnace wall and insulation layer coverage area, IJ is the interlayer area, and JA is the outer wall covering insulation layer area. To obtain accurate temperature boundary conditions for each drum area, 10 thermocouples were arranged on the internal and external drum walls. The temperature boundary condition of a given area was determined based on the temperature value obtained from each thermocouple. As the tube part is directly exposed to the flame or high-temperature flue gas, its operating environment is harsh, and the temperature value cannot be directly obtained from the thermocouple. Therefore, the temperature boundary conditions of the tube part were estimated based on engineering experience[7]. As the self-weight of the working medium in the drum is ignored, the pressure boundary conditions of the inner wall of the drum and the tube are assumed to be equal to the pressure value in the saturated state of the working medium. The boundary conditions of each area are shown in **Table 1**.

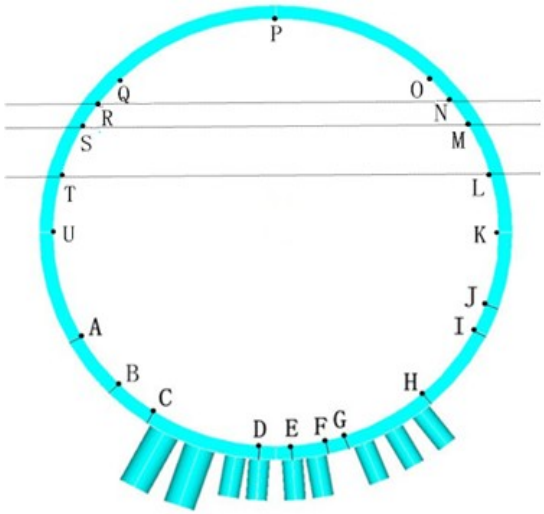

Fig. 4 Division of heat transfer area

Table 1 Boundary conditions of the drum wall and tubes

Load position	Boundary conditions	Load position	Boundary conditions
Inner surface AB	$T = 194.0\,^{\circ}\mathrm{C}$	Outer surface AB	$h = 4.2\,\mathrm{W/(m^2 \cdot K)}, T_f = 61.3^{\circ}\mathrm{C}$
Inner surface BC	$T = 194.2\,^{\circ}\mathrm{C}$	Outer surface BC/ FG	$q = 0\,\mathrm{J/(m^2 \cdot s)}$
Inner surface CD	$T = 192.1\,^{\circ}\mathrm{C}$	Outer surface CD/ EF	$T = 192.1\,^{\circ}\mathrm{C}$
Inner surface DG	$T = 193.9\,^{\circ}\mathrm{C}$	Outer surface DE	$T = 211.2\,^{\circ}\mathrm{C}$
Inner surface GI	$T = 194.7\,^{\circ}\mathrm{C}$	Outer surface GI	$T = 196.1\,^{\circ}\mathrm{C}$
Inner surface IK	$T = 193.3\,^{\circ}\mathrm{C}$	Outer surface IJ	$h = 4.4\,\mathrm{W/(m^2 \cdot K)}, T_f = 61.3^{\circ}\mathrm{C}$

Inner surface KU	$T = 194.4\,°C$	Radiation zone tube	$T_{in} = 191.97\,°C, T_{out} = 251.97\,°C$
Inner surface UA	$T = 193.3\,°C$	Convection zone tube	$T_{in} = 191.97\,°C, T_{out} = 221.97\,°C$
Inner surface JA	$T = 192.5\,°C$	Downcomer	$T_{in} = 181.97\,°C, T_{out} = 181.97\,°C$
Internal pressure of drum	$P = 1.21\,MPa$	Internal pressure of tube	$P = 1.21\,MPa$

5 Results and discussion

5.1 Mesh independence verification

To improve the efficiency of mesh division of the supercharged boilers and reduce the overall number of meshes, reasonable segmentation was carried out for different parts of the drum during the modeling process. As the stress value in the orifice plate of the drum is the main focus of attention, the pipe holes were locally refined. The mesh distribution of the drum and the tube is shown in **Fig. 5**. Considering that the mesh in other areas is reasonable, the size of the mesh in the orifice area was changed to obtain a curve of the stress value at the danger point using a large number of meshes, as shown in **Fig. 6**. Finally, the mesh size of the orifice plate area was determined to be 2.5 mm, the thickness of the orifice plate was divided into 5 layers, and the overall mesh number of the solid model was 2974915.

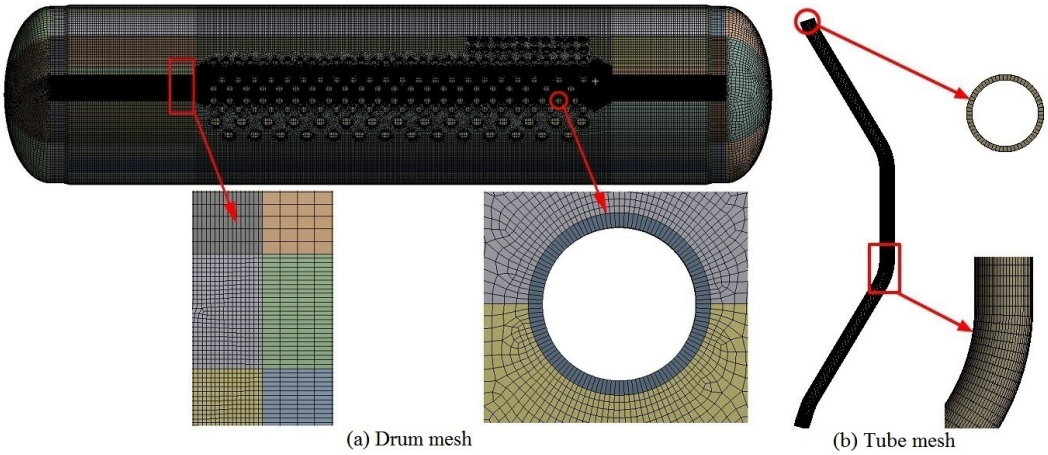

(a) Drum mesh (b) Tube mesh

Fig. 5 Mesh division

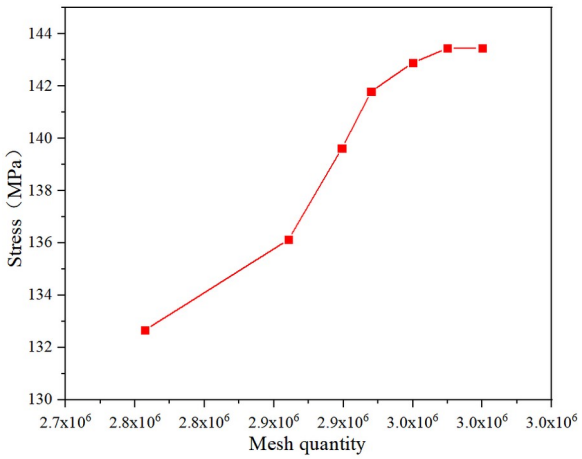

Fig. 6 Mesh independence verification

To ensure a reliable comparison between the simplified model and the solid model, the mesh setting of the simplified model was kept consistent with that of the solid model, and the modeling mode of the tube was the only variable. **Fig. 7(a)** and **(b)** show the mesh distribution of the simplified model composed of solid and beam elements, wherein the number of meshes is 2302974815 and 964875, respectively. The solid model drum and tube mesh accounted for 25.6% and 23174.4%, respectively. Although it is important to maintain a reasonable mesh number for the tubes, 232the influence of the tubes on the stress distribution of the drum cannot be ignored. Therefore, the 233mesh number of the tube must be reduced while ensuring the integrity of the structure and the 234reliability of the results.

The simplified model based on beam elements proposed herein can better solve the above 236research difficulties, and the mesh number can be increased to optimize the drum, to improve the 237accuracy and efficiency of the calculation results. As shown in **Fig. 7(b)**, the simplified beam 238element model requires a significantly lower mesh number. Moreover, the proportion of the 239meshes in the drum and the tubes is reversed, thereby reducing the overall mesh number. The 240specific calculation efficiency and reliability of the result is analyzed in the subsequent finite 241element analysis.

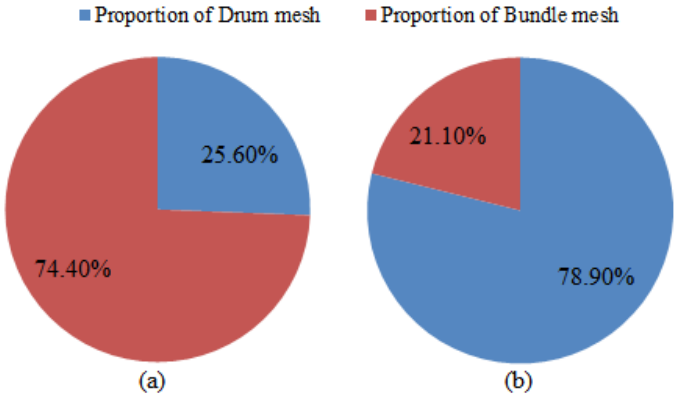

Fig. 7 Mesh distribution of finite element model

2435.2 Calculation results of solid tube model

Fig. 8(a) and **(b)** show the overall temperature and coupling stress distribution, respectively, 245of the supercharged boiler. As shown, there is a significant difference in the distribution of the

stress and temperature fields in the drum area, which indicates that the coupling stress of the drum area is more significantly affected by the mechanical stress due to the pressure difference between the interior and exterior of the drum. Considering the tubes, the stress distribution is consistent with the temperature distribution trends; the higher the temperature, the higher the stress. This is because the exterior of the tube is directly washed by the furnace flame and flue gas, whereas the temperature of the internal working fluid is relatively low, thereby resulting in a large temperature difference between the interior and the exterior of the boiler. Therefore, the thermal stress is dominant near the tube area. Therefore, during the design process of a supercharged boiler, a material with high tensile strength should be selected for the drum, and a material with good thermal conductivity should be selected for the tube.

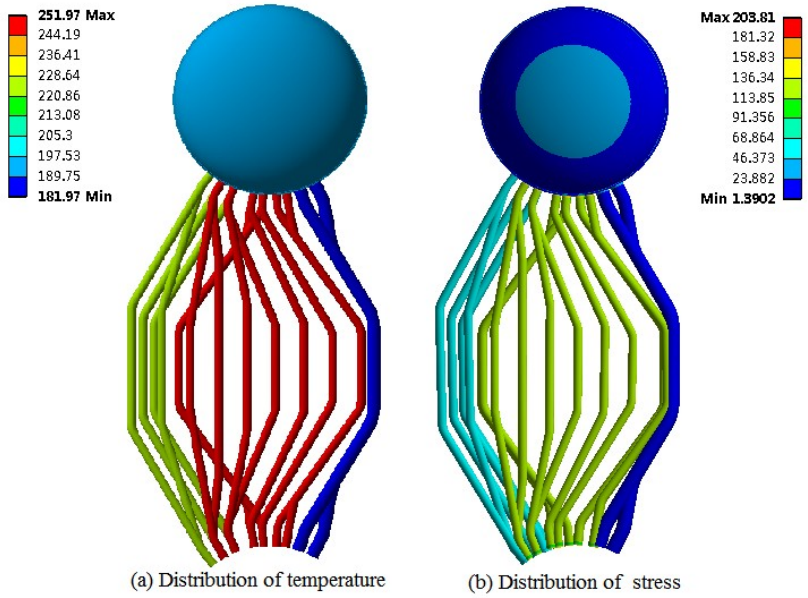

Fig. 8 Temperature and stress distribution

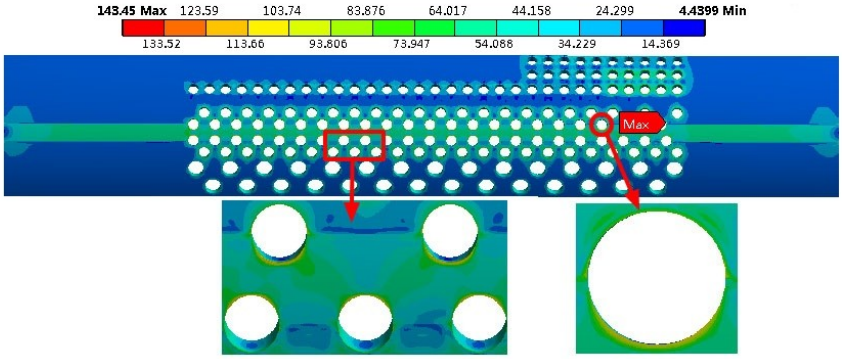

Fig. 9 Solid model orifice plate stress distribution

Fig. 9 shows the distribution of the coupling stress at the orifice plate of the drum. As shown, the stress at the edge of the tube hole is relatively large, and the danger point occurs at the edge of the first row of the tube holes in the radiation zone. This is because the openings destroy the continuity of the shell material and weaken the original bearing area. And the existence of the nozzles makes the nozzle opening area a discontinuous area in the overall structure. consequently, stress concentration inevitably occurs near the edge of the openings. In addition, the shell and the nozzle area are inconsistent during free deformation due to the internal pressure, and edge stress is

generated during the deformation coordination process. Furthermore, as the tubes are arranged asymmetrically along the axial direction of the drum, the entire structure is biased towards the right end of the drum. Consequently, the tubes on both sides of the drum experience an uneven amount of force and higher mechanical stress. In addition, a significant temperature difference exists between the contact portion of the tubes and the orifice plate, which produces a large thermal stress in the connection area. Moreover, the radiation area experiences higher temperatures and thermal stress, due to which the danger point occurs at the edge of the radiation area.

As shown in **Fig. 9**, the stress of the oblique hole bridge is higher than that of the axial hole bridge, and the circumferential stress of the drum at the pipe holes is higher than the axial stress. The results demonstrate that the tubes have a significant effect on the circumferential force between the tubes and the drum during the actual operation of the boiler. This is because the number of tubes in the axial position of the orifice plate is significantly higher than that in the circumferential direction. Furthermore, the relative height of the tubes in the circumferential direction and the orifice plate in the contact position varies, increasing the likelihood of the circumferential rotation of the drum owing to uneven forces in the circumferential direction. Consequently, the circumferential stress is significantly higher than the axial stress. The two sides of the radiation area are the downcomer and the convection pipe. The temperature changes significantly along the circumferential direction of the drum, resulting in a higher thermal stress. In contrast, the temperature change along the axial direction is relatively uniform, and the thermal stress is small, further increasing the difference between the circumferential stress and the axial stress on the drum.

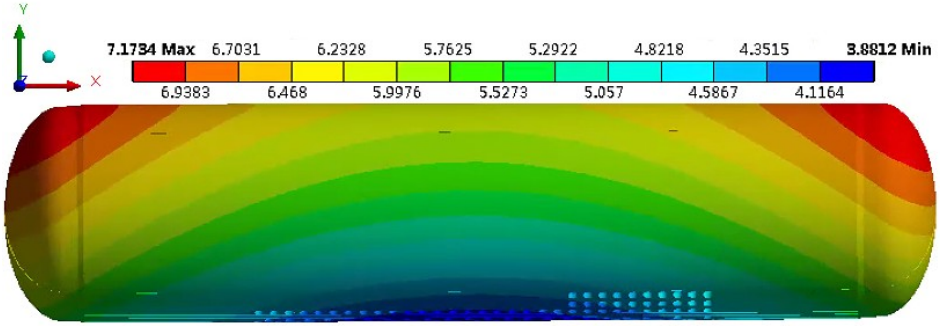

Fig. 10 Solid model drum displacement distribution

Fig. 10 shows the overall displacement distribution of the drum. As shown, the displacement distribution extends from the bottom center of the drum, scalloped on both sides, and the tops of the two sides correspond to the maximum displacement position. At these points, the displacement values in the X, Y, and Z directions are 3.88 mm, 6.28 mm, and 2.40 mm, respectively. According to linear elasticity theory and superposition principle, the displacement of the model is influenced by the coupling stress caused by the temperature difference and internal pressure of the drum, and is proportional to the size of the component. As the internal pressures of the drum and the tubes in this model are uniform, the thermal stress due to the temperature difference becomes the decisive factor that determines the relative displacement of the drum in each direction. Considering the changes in the dimensions of the model in various directions, the drum displacement shows a decreasing distribution trend along the Y, X, and Z directions. The displacement vectors in each direction are superimposed to obtain the distribution law shown in **Fig. 10**.

5.3 Simplified model evaluation

The overhang length of the solid tubes was varied to obtain an optimal simplified model. Furthermore, the stress and displacement results of the solid model were used as evaluation indicators to verify the reliability of the calculation results of the simplified model.

The tubes are connected to the drum through the orifice plate, and the interaction at the interface between the two is an important factor that affects the stress of the drum. However, it is impossible to replace all the solid tubes with beam element tubes during the actual model simplification process as this increases the complexity of applying the beam–solid contacts. Therefore, to simplify the structure as much as possible, the influence of the overhang length of the solid bundle must be studied. During the model verification stage, the volume and structure of the original model were reduced by some extent to improve the computational efficiency. As shown in **Fig. 11(a)**, the number of meshes in the reduced model was only one-third of that in the original model. **Fig. 11(b)** shows the variation in the coupling stress and displacement of the drum with the increase in the overhang length of the tubes. As the overhang length increases, the model displacement varies by less than 2.5%. When the overhang length is above 12 mm, the stress varies by less than 0.4%. Therefore, when the overhang length is above 12 mm, its influence on the stress and displacement can be ignored. Finally, to ensure the convenience of modeling, the straight pipe section of the tube was retained as a solid tube, and the other parts were replaced by beam elements, as shown in **Fig. 3**.

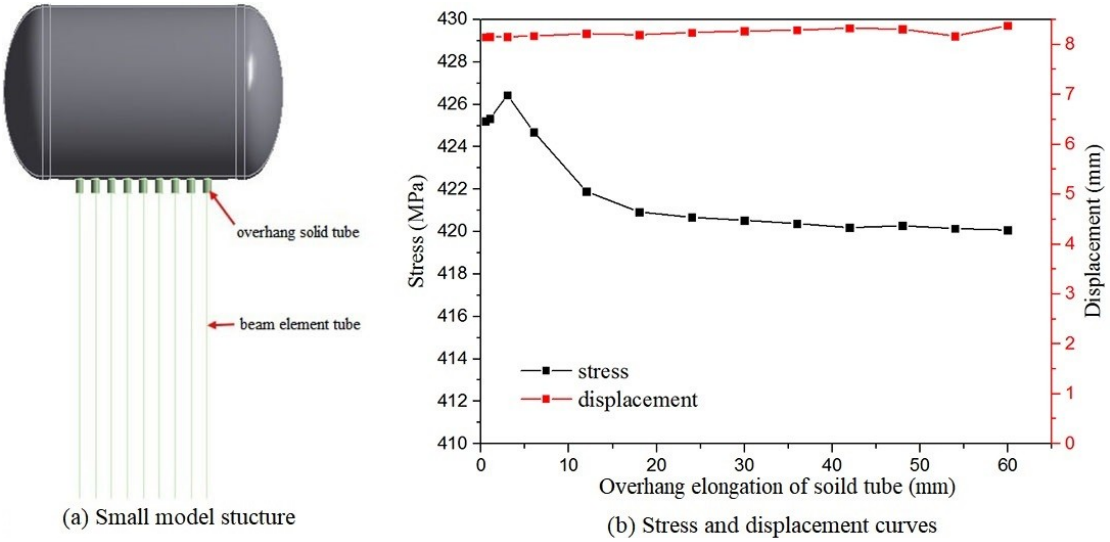

Fig. 11 Small model study

Table 2 Comparison of calculation results

Structure type	Danger point	Stress (MPa)	Displacement (mm)	Mesh number		Computation Time (s)	
Solid model	Radiation area: 1 row and 1 column	143.45	7.17	2974815		1087	
Simplified model		148.39	6.80	976035		347	
Maximum relative error		3.44	5.16	Mesh Quantity	−67.19	Computation	−68.08

(%)			Rate (%)		Rate (%)	

Fig. 12(a) depicts the stress distribution of the simplified model. As shown, the stress distribution trend and the position of the danger point at the orifice plate are consistent with those of the solid model, and the maximum relative error is 3.44%. **Fig. 12(b)** shows the corresponding displacement distribution. As shown, the displacement distribution trend of the simplified model is the same as that of the solid model. Both models are characterized by a fan-shaped expansion from the center of the bottom of the drum to both sides of the drum. The tops of the sides of the head are the maximum displacement positions, and the maximum relative error, as shown in **Table 2**, is 5.16%. This error is primarily due to two reasons: (1) The solid tube is a surface constraint, and the beam element tube is a point constraint; consequently, there is a slight difference in the moment of inertia between the two; (2) The beam element based on the Timoshenko beam theory cannot exhibit significant section deformation near the beam node or the beam–solid interface[12].

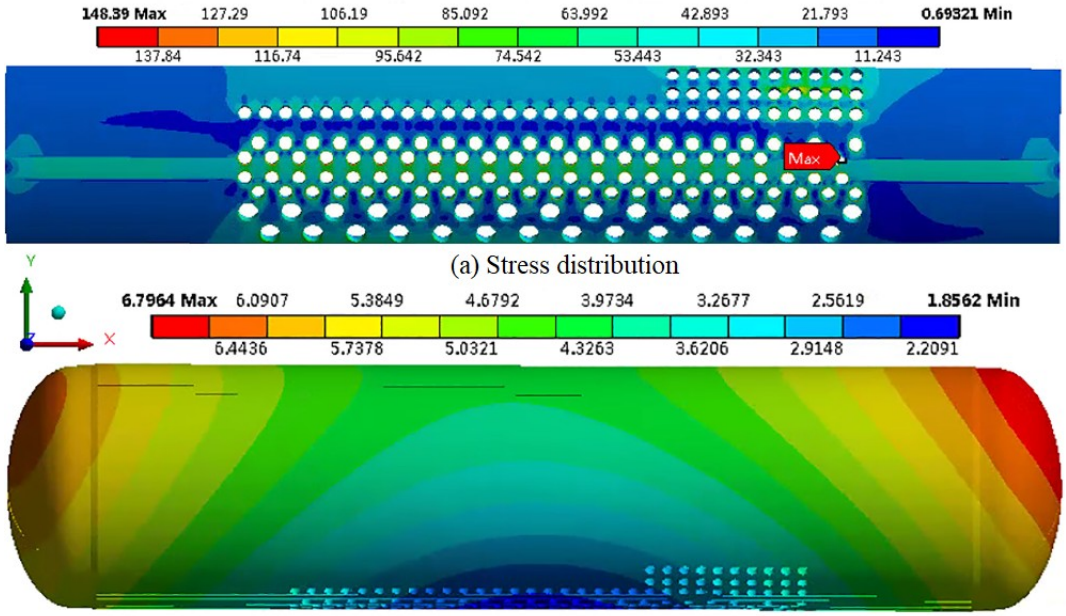

(a) Stress distribution

(b) Displacement distribution

Fig. 12 Simplified model study

In addition to ensuring the reliability of the calculation results, improving the efficiency of the model simulation calculation is the focus of this study. Compared to the solid model mesh, the overall mesh number of the simplified model is 67.19% lower, the mesh number of the tube bundle is 90.30% lower, and the calculation time is 68.08% lesser, as shown in **Table 2**. Therefore, this method simplifies the structural analysis calculation of supercharged boilers significantly. Furthermore, it can also be extended to relevant structural analyses of various tube heat exchangers and pressure vessels, effectively reducing simulation calculation costs and conserving resources.

5.4 Fatigue life assessment system of drum

Numerous pipe holes are distributed in the orifice plate of the drum, leading to stress concentration in this area and making it prone to fatigue damage. Most scholars consider the danger point as the fatigue life check point to calculate the fatigue life of the drum. However, transient simulation results indicate that the position of the danger point is not necessarily the

position of the maximum stress amplitude, and is instead affected by several factors. Therefore, the fatigue life assessment of a supercharged boiler drum based solely on the stress value at the danger point is one-sided. Moreover, the fatigue of supercharged boiler drums is low-cycle fatigue, and the life of low-cycle fatigue is dispersed. Consequently, in this study, we apply statistical methods to the fatigue life assessment of supercharged boiler drums.

The orifice plate of the drum considered herein has 170 holes. The maximum stress amplitude at the edge of each pipe hole was calculated using the third strength theory and the fatigue life of each point was $1.25\times10^{9}-5.15\times10^{24}$ based on the ASME standard. The fatigue life of each point, under the same operating conditions, has significant dispersibility, which demonstrates that using the fatigue lives corresponding to the danger points as the overall model is not scientific and rigorous. Therefore, we use a statistical fatigue life analysis method instead of a deterministic fatigue life analysis method to evaluate the fatigue life of the boiler drum. The feasibility of this method has been proved in numerous application scenarios[18-22]. The fatigue life of the drum is a random set of data. Therefore, it is first necessary to determine the distribution function of the data.

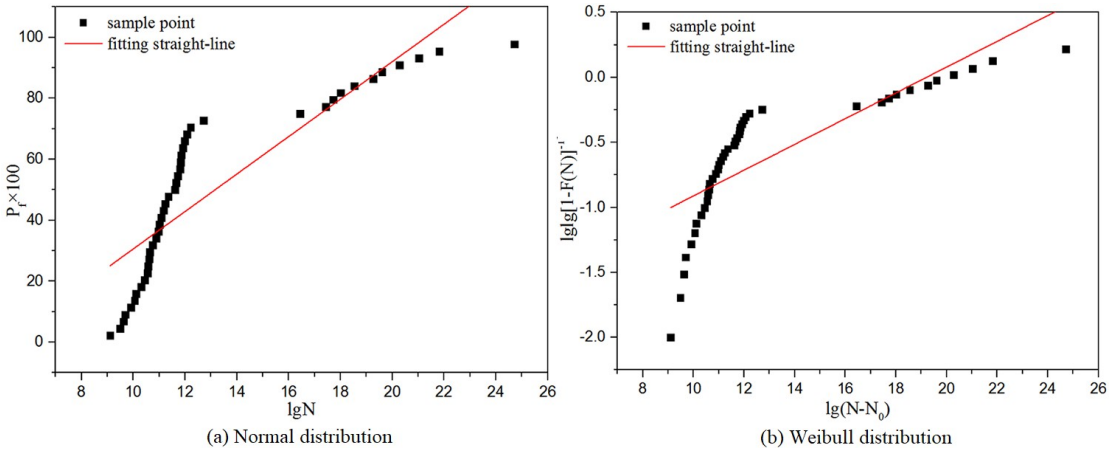

Fig. 13 Distribution function decision

Two commonly used distribution functions in statistical fatigue analyses are Weibull distribution and normal distribution. The most suitable distribution function is determined as follows.

If a linear relationship with $\lg\left[1-F\left(N\right)\right]^{-1}$ and $\lg(N-N_0)$ as the vertical and horizontal coordinates exists, it obeys the Weibull distribution; if a linear relationship between $\lg N$ and P_f as the vertical and horizontal coordinates exists, then N follows the normal distribution. P_f represents the average rank estimator of the probability of material damage and is calculated as: $P_f=i/(n+1)$, where n is the number of sample points, and $F(N)=P_f$.

A total of 43 sample points were obtained from the fatigue data, and the above criteria were used for the statistical analysis to obtain the relationship curves shown in **Fig. 13(a)** and **Fig. 13(b)**. To further determine the reliability of the linear relationship, linear regression analysis was used to obtain correlation indices of the normal and Weibull distributions, which were equal to 0.74 and 0.62, respectively. The results demonstrate that the calculated fatigue data satisfy the

normal distribution and Weibull distribution, but are better characterized by the normal distribution.

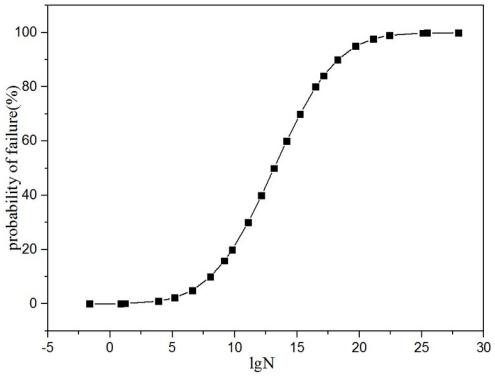

Fig. 14 Logarithmic fatigue life and failure probability curve

The normal distribution was used to obtain the relationship between the logarithmic fatigue life and the failure probability, as shown in **Fig. 14**. The results indicate that under the current working conditions, when the fatigue life of the drum is $10^5 - 10^{20}$, the stress change in the orifice plate area has a higher impact on the fatigue life. When the stress amplitude of the drum is $24 - 148\,\mathrm{MPa}$, the increase in the stress amplitude significantly increases the probability of the fatigue failure of the drum. Therefore, the fatigue life calculation should focus on the stress amplitude within this range. When the fatigue life $N < 10^5$ or $N > 10^{20}$, maximum and minimum values of fatigue life exist, which correspond to an almost unchanged probability of failure. Moreover, this area also appears as a small probability event area for fatigue failure, which is consistent with the actual situation. Thus, the logarithmic fatigue life and failure probability curve established herein can effectively improve the accuracy of fatigue life prediction under low-cycle fatigue and increase the reliability of simulation calculations. It can provide technical support for fatigue life calculation and failure prediction under various operating conditions.

Conclusion

Supercharged boilers have complex structures and performing finite element structural analyses using complete models is costly. Therefore, a simplified modeling method that uses beam elements in place of solid tubes was proposed herein. The proposed method can significantly improve the calculation efficiency and reduce calculation costs, while ensuring structural integrity and accurate results. In addition, considering factors such as the dispersion of low-cycle fatigue life, a statistical approach was used to evaluate the fatigue life of the drum. The point of maximum stress amplitude at the edge of each pipe hole was used as the fatigue life check point, and the failure probability of each fatigue life was calculated by combining statistical methods. This approach improves the fatigue life evaluation of supercharged boiler drums, and increases the accuracy of fatigue life prediction and the credibility of the simulation calculations. The main conclusions are as follows.

(1) Stress concentration occurs at the edge of the orifice, the stress along the circumference of the drum is higher than the axial stress, and the danger point occurs in the first row of the right side of the radiation area.

(2) The overhang length of the solid tube has a minimal effect on the displacement of the drum; when the external elongation is 12 mm, its influence on the stress of the drum is negligible.

(3) The simplified method can reduce the overall mesh number of the model by 67.19%, the mesh number of the tube bundle by 90.30%, and the calculation time by 68.08%. The maximum

relative errors of stress and displacement were 3.44% and 5.16%, respectively.

(4) For a fatigue life of $10^5 - 10^{20}$, the failure probability of the drum varies significantly. When the stress amplitude of the drum is $24 - 148\,\mathrm{MPa}$, an increase in the stress amplitude significantly increases the probability of fatigue failure of the drum. Consequently, the fatigue life calculation should focus on the stress amplitude within this range. When the fatigue life $N < 10^5$ or $N > 10^{20}$, the corresponding fatigue failure probability remains almost unchanged, and the area is a small probability event area for fatigue life.

Nomenclature

α	Linear expansion coefficient of material，1/K
E	Modulus of elasticity，MPa
Δt	Temperature difference，℃
μ	Poisson's ratio
K	Ratio of outer radius to inner radius of drum
K_r	Ratio of outer radius to any radius of drum
σ_r^t	Radial thermal stress, MPa
σ_θ^t	Axial thermal stress, MPa
σ_z^t	Tangential thermal stress, MPa
r_1, r_2	Inner and outer radius of drum，mm
p_i, p_o	Interior and exterior pressure of drum, MPa
σ_r^s	Radial mechanical stress, MPa
σ_θ^s	Axial mechanical stress, MPa
σ_z^s	Tangential mechanical stress, MPa
L	Length, mm
G	Shear modulus, MPa
A	Cross-section area, mm^2
ω	Non-uniform shear coefficient of cross-section
v	Deflection, mm
θ	Bending angle, rad
γ	Shearing angle, rad
S_a	Alternating stress amplitude, MPa
Y	Material constant used for the fatigue knock-down factor
X	Material constant used for the fatigue knock-down factor
N	Permissible number of cycles

u_i	Slave the degree of freedom
u_j	Master degrees of freedom
C_j	Weight coefficient
C_0	Constant term
i	Subscript, some degree of freedom from the node
j	Subscript, some degree of freedom of the master node
P_f	The average rank estimator of the probability of material damage
n	Number of samples
i	The number of fatigue life from small to large

412

413**References**

414[1]Xie Z J, Feng H J, et al. Constructal design for supercharged boiler evaporator[J]. International
415Journal of Heat and Mass Transfer. 2019, 138(8): 571-579.
416[2]Ming P J, Sun B Z, Li Y J, et al. Research on marine boiler's pressurized combustion and heat
417transfer[J]. Journal of Thermal Science, 2005, 14(1):76-80.
418[3]Saha A, Roy H, Ray S, et al. Author's personal copy Investigation of probable cause of damage
419of steam drum of naphtha cracking furnace[J]. Engineering Failure Analysis, 2009, 16(5):1387-
4201396.
421[4]Juan C P A, Guillermo E O C, et al. Thermome-chanical analysis of the drum of a steam
422generator using the finite element method[J]. Journal of Process Mechanical Engineering. 2012,
423227(3): 157-165.
424[5]Majcher A, et al. Stress analysis for the start-up operation on the example of op-210 boiler
425drum[J], Problemy Eksploatacji-Maintenance Problems. 2013, 2: 19-28.
426[6]Okrajni J, Twardawa M. Description of the thermo-mechanical fatigue of thick-walled pressure
427vessels[J]. Procedia Materials Science, 2014, 3(6): 918-923.
428[7]Zeng Q P, et al. Fatigue life analysis of supercharged boiler based on the design by analysis
429method [J]. International Journal of Pressure Vessels and Piping 188.
430[8]Sreenath S, Saravanan U, Kalyanaraman V. Beam and shell element model for advanced
431analysis of steel structural members[J]. Journal of Constructional Steel Research, 2011,
43267(12):1789-1796.
433[9]Adam J S, On the advantages of hybrid beam-shell structural finite element models for the
434efficient analysis of metal wind turbine support towers[J] , Finite Elements in Analysis and
435Design, 2019, 162(5): 19-33.
436[10]Lee S, Kim S. Simplified beam model of high burnup spent fuel rod under lateral load
437considering pellet-clad interfacial bonding influence[J]. Nuclear Engineering and Technology,
4382019, 51(3):1333-1344.
439[11]Kim J S, Kim J Y. Simplified Elastic-Plastic Analysis Procedure for Strain-Based Fatigue
440Assessment of Nuclear Safety Class 1 Components under Severe Seismic Loads[J]. Nuclear
441Engineering and Technology, 2020.
442[12]Nguyen N L, Jang G W, Choi S, et al. Analysis of thin-walled beam-shell structures for
443concept modeling based on higher-order beam theory[J]. Computers & Structures, 2018, 195:16-

33.
[13]Vinot P, Conan S, Piranda J. Shape optimization of thin-walled beam-like structures[J]. Thin Walled Structures, 2001, 39(7): 611-630.
[14]Jang G W, Kim Y Y. Higher-order in-plane bending analysis of box beams connected at an angled joint considering cross-sectional bending warping and distortion[J]. Thin Walled Structures, 2009, 47(12):1478-1489.
[15]Cas B, Planinc I, Schnabl S. Analytical solution of three-dimensional two-layer composite beam with interlayer slips[J]. Engineering Structures, 2018, 173(15): 269-282.
[16]ASME Boiler and Pressure Vessel Code.Section VIII.rules for construction of pressure vessels,division 2.New York:ASME:2017
[17]Jendele L, Cervenka J. On the solution of multi-point constraints – Application to FE analysis of reinforced concrete structures[J]. Computers & Structures, 2009, 87(15-16): 970-980.
[18]Li Z, Xue Z, Wang X, et al. Safe life estimation of coke drum in service environment [J]. Journal of Pressure Vessel Technology, 2012, 134(3): 031601.
[19]Dunand-Chatellet C, Moumni Z. Experimental analysis of the fatigue of shape memory alloys through power-law statistics[J]. International Journal of Fatigue, 2012, 36(3):163-170.
[20]Bag A, Delbergue D, Bocher P, et al. Statistical analysis of high cycle fatigue life and inclusion size distribution in shot peened 300M steel[J]. International Journal of Fatigue, 2018, 118(1): 126-138.
[21]Gaurav A, Singh K K. Effect of pristine MWCNTs on the fatigue life of GFRP laminates-an experimental and statistical evaluation[J]. Composites, 2019, 172(9): 83-96.
[22]Yan Z, Zhang Y, Chen J, et al. Statistical method for the fatigue life estimation of coke drums[J]. Engineering Failure Analysis, 2015, 48(2): 259-271.